Laser and Particle Beams (2012), *30*, 357–367.

doi:10.1017/S0263034612000195

The effect of intense short pulse laser shapes on generating of the optimum wakefield and dissociation of methane molecule

E. IRANI, S. ZARE, H.A. NAVID, Z. DEHGHANI, AND R. SADIGHI-BONABI
Departments of Physics, Sharif University of Technology, Tehran, Iran
(RECEIVED 27 November 2011; ACCEPTED 14 March 2012)

Abstract

The optimum convolution of dual short pulse for producing the maximum wakefield and the highest dissociation probability of CH_4 has been investigated. By using three fundamental shapes of pulses though four different arrangements, the generated wake are considered in plasma. It is found that when the first and second pulses were rectangular–triangular and sinusoidal pulse shapes, respectively, the resultant wakefield amplitude is the highest. This effect opens up a new novel way by pulse shaping mechanism in the photo dissociation dynamics of molecules and controlling of chemical reactions in the desired channels by short pulse intense lasers for reducing the computation time of genetic algorithm model. Using field assisted dissociation model, the dissociation probability for a CH_4^+ molecule exposed to a 100 femtosecond 8 Jcm^{-2} Ti:Sapphire laser pulse is calculated. Here, the highest possible dissociation probability of the methane ion is calculated by the gradient optimization method in which the gradient of a function should be in the direction of the local extremes. The C-H molecular bond of CH_4^+ ion is assumed to be in the same direction as the electric field component of the laser pulse. These results show that there is an excellent match with experimental data. The remarkable feature of this work is that the sensitivity of the dissociation probability of the initial bond length q, is studied and the desired product channel is controlled by variation of the laser intensity and it's time evolution by introducing a characteristic vectored space for intensity and duration of two tailored rectangular femtosecond laser pulses.

Keywords: Intense short pulse laser; Methane molecule; Pulse shaping; Wakefield

INTRODUCTION

The continuous rapid advance in the development of ultra-intense short pulse lasers stimulated the realistic expectation of using such devices in producing energetic particle beams for application in various fields. The laser-matter interaction meets the high energy physics in laser-plasma accelerators in generating highly collimated bright X-ray and γ sources (Giulietti *et al.*, 2005; Chyla, 2006; Bessonov *et al.*, 2008; Maslova *et al.*, 2008). Ion blocks of many vacuum wavelength thickness are produced and moved in the direction of the emitted short laser pulses (Glowacz *et al.*, 2006; Yazdani *et al.*, 2009; Hora, 2009; Sadighi-Bonabi *et al.*, 2010*a*, 2010*b*). Among the different options, recently, much attention is focused on the possibilities of laser transmutation by highly directional γ-beams generated from ultra-intense short pulse lasers (Sadighi-Bonabi *et al.*, 2006; 2010*c*; 2010*d*). These lasers are also used to generate a quasi-Maxwellian and quasi-mono-energetic electron beams (Malka & Fritzler, 2004; Glinec *et al.*, 2005). Recent introduced ellipsoidal bubble regime has also demonstrated the generation of high-quality and low divergence electron bunches with very high energies in relatively small energy spread (Sadighi-Bonabi *et al.*, 2009*a*, 2009*b*, 2009*c*, 2010*e*, 2010*f*; Zobdeh *et al.*, 2008, 2010). These lasers gave researchers the ability to produce electrons with energy of more than the conventional accelerators (Hora, 2004, 2007; Roth *et al.*, 2005; Liu, 2009). Currently, in plasma based acceleration, electrons with a phase velocity up to the speed of light driven by an intense laser beam can be obtained (Dyson & Dangor, 1991; Sadighi-Bonabi *et al.*, 2010*e*, 2010*f*). The propagation of such intense laser field and related focusing parameters in plasma with

Address correspondence and reprint requests to: R. Sadighi-Bonabi, Department of Physics, Sharif University of Technology, 11365-9161 Tehran, Iran. E-mail: sadighi@ sharif.ir

various density profiles is investigated in the various plasma conditions (Sadighi-Bonabi *et al.*, 2009*d*, 2010*g*, 2010*h*). More recently these monoenergetic electron beams are used to produce more intense X-ray beams (Nikzad *et al.*, 2012). The extremely high electric field makes the Laser WakeField Acceleration (LWFA) method attractive for the development of a new generation of accelerators and improving the scaling up to GeV energies in compact laser plasma accelerators (Lifschitz *et al.*, 2006).

Rosenzweig *et al.* (1988) reported the first experimental observation of the plasma wakefield. By enhancing the interaction length of the laser pulse with the plasma such as trapping plasma in channels, one can obtain greater amplitude wakefields (Cros *et al.*, 2000; Sprangle, 2001). Wakefield can also be created by relativistic electron bunches (Balakirev *et al.*, 2001). The phenomenon of generation of wakefield using a sinusoidal seed laser pulse and another coaxially propagating sinusoidal shape trailing pulse is reported (Gaurav *et al.*, 2008). Modern chemistry made the dreams of converting and controlling the motion of molecules transparent, in order to drive a chemical reaction into a desired thermally inaccessible state by a light and laser pulses experimentally (Judson & Rabitz, 1992; Bostandoust Nik *et al.*, 2010). This old dream of understanding the dynamics of chemical bonds soon became reality by real-time observations of the transition-state region between reagents and products (Zewail, 1988). This important idea was translated from theory to a unique experiment by Judson and Rabitz (1992). They introduced a laser system whose pulse sequence was supplied by a computer equipped with the genetic algorithm code. Since then, femtosecond pulse shaping became a powerful tool in coherent control of chemical reactions. By using femtosecond lasers, it is now possible to record snapshots of chemical reactions with sub-Angstrom resolution (Assion *et al.*, 1998*a*, 1998*b*; Bauer *et al.*, 2003), multiphoton transitions (Bauer *et al.*, 2002), coherent anti-stokes Raman spectroscopy and high harmonic generation (Oron *et al.*, 2003; Bauer & Ceccherine, 2001). Considerable efforts have been made toward the realization of coherent control of chemical reaction by using laser pulse shapers through the coherent control, which is based on the manipulation of wave packets to a desired reaction channel (Hornung *et al.*, 2000; Graham *et al.*, 2000, 2003; Sugimori *et al.*, 2007). Fundamental theories for pulse shaping involve solving a time-dependent variation method to optimize the performance index related to a reaction of interest. If $|\psi(t)>$ and $|\psi_{target}>$ denote the wave function and the desired chemical channel, respectively, in an optimal coherent control one should find the proper laser pulse electric field $E(t)$, so that $|<\psi_{target}(t)|\psi(t)>|^2$ is maximized (Rabitz *et al.*, 1988; Breuer *et al.*, 1992; Brumer & Shariro, 2009). In this condition, one needs to solve the complicacy in the molecular Hamiltonian and time dependent Schrodinger equation. Based on the Judson and Rabitz (1992) report, by combining the pulse shaping techniques with genetic and learning algorithms, one can find tailored pulses for proper controlling the chemical reactions. Although, great improvements are achieved in controlling chemical reactions by these methods, initial experimental data for genetic and learning is needed. Solving the complicated time dependant Schrodinger equation and the problems related to design an appropriate field requires full knowledge of the molecular Hamiltonian, which is not very well known for polyatomic molecules. Moreover, the theoretically designed approximate fields do not always take into account the errors introduced by apparatus in the laboratory (Castro & Gross, 2009; Jiang *et al.*, 2005; Oron & Silberg, 2005). Many applications of these systems have been motivated by recent advances on ultrafast high power lasers. Deeper knowledge on the propagation of high intensity laser beams and related focusing parameters in plasma with various density profiles has been obtained (Cowan *et al.*, 1999; Hoffmann *et al.*, 2005; Sadighi-Bonabi *et al.*, 2009*a*).

The aim of this study is to observe the effect of wakefield amplification by various shapes of the laser pulses propagated in plasma. A detailed analytical study of a unique idea of wakefield amplification by two laser pulse shapes with copropagating one behind the other, with a fixed distance between them is reported. The laser pulses are considered to have the same moderate intensities, polarizations and frequencies propagating in cold, uniform, unmagnetized, and under-dense plasma. Starting from Maxwell equation, dispersion relation for the laser propagation in the plasma is obtained and the optimum two combined short laser pulses are introduced. Furthermore, in this work, we introduce a simple, reproducible, and unique method to find the optimum two tailored rectangular short laser pulses for controlling the methane ion dissociation numerically. The shape of the pulse with qualified and introduced parameters is now capable to cover the other transitions for several possible pathways, properly. In the present model, the structural complicacy of solving the related time dependant Schrodinger equation does not exist and the obtained relative yield of the fragment ions is achieved more than the total quantum yield. This method can have a significant contribution in prediction of the optimum shaping of short laser pulses for dissociation of molecules. In this efficient and low cost method, without requiring experimental data, an optimum pulse shape with the maximum probability of dissociating polyatomic molecules are introduced. For finding the dissociation probability, an investigation has been made in the methane ion dynamics during its interaction with defined femtosecond laser pulses.

THE MODEL

In the interaction of a laser pulse with plasma, the related ponderomotive force separates electrons and ions. These charged particles attract together by electrostatic Coulomb force and this leads to electron oscillation at the plasma frequency $\omega_p = (4\pi e^2 n_0/m)^{1/2}$, with n_0, m, and e are the density of plasma electrons, the rest mass of electron and the electron charge, respectively. In this study, the wakefield is generated

https://doi.org/10.1017/S0263034612000195 Published online by Cambridge University Press

by a laser pulse with frequency ω_0, intensity I_0, duration τ, and pulse length $L \sim \lambda_p$ (where λ_p is the plasma wavelength). It is assumed that the laser pulse propagates in cold, homogenous, under-dense, and uniform preionized plasma, in which collisions and ion dynamics are neglected. It should be realized that when pulse lengths are near the plasma wavelength, then the relativistic self-focusing of the laser beam can be ignored in the plasma; therefore, due to relativistic nonlinearity the pulses will propagate more than a Rayleigh length without undergoing any significant distortion (Sprangle *et al.*, 2001; Leemans *et al.*, 2002; Sadighi-Bonabi *et al.*, 2011). In the present work for avoiding the self-focusing, the minimum spot size of the laser beam assumed to be much larger than the plasma wavelength $r_0 >> \lambda_p$ and in this condition one-dimensional model is used (Sprangle *et al.*, 1990; Gaurav *et al.*, 2008).

The electric field of the laser pulse is assumed as following:

$$\vec{E} = \hat{x}E_0 \cos\{k_0 z - \omega_0 t\}, \tag{1}$$

E_0, ω_0, and k_0 represent the amplitude, frequency, and propagation constant, respectively. E and E_0 are functions of time t, position z, and radial distance r.

Starting from the Maxwell equations for a linearly polarized laser beam along x-axis and considering a weakly relativistic case, the following fluid equations can be used.

$$m\left(\frac{\delta\vec{v}}{\delta t} + (\vec{v}.\nabla)\vec{v}\right) = -e(\vec{E} + \vec{E}_w) - \frac{\vec{v}}{c} \times e(\vec{B} + \vec{B}_w), \tag{2a}$$

$$\frac{\delta n_e}{\delta t} + \nabla.(n_e\vec{v}) = 0, \tag{2b}$$

$$\vec{\nabla}.\vec{E} = -4\pi e(n_e - n_0), \tag{2c}$$

$\vec{v}$ and c are the velocity of the plasma electrons affected by laser field and light velocity, respectively. The electron density is assumed as $n_e = n_0 + n_i$, where n_e and n_0 are the perturbed and unperturbed density (a weakly nonlinear regime $n_i << n_0$, is considered). In Eq. (2) $\vec{E}$, $\vec{B}$, and $\vec{E}_w$, $\vec{B}_w$ represent electric, magnetic field vector of the laser pulse and electric, magnetic field of wakefields, respectively.

New variables $\zeta = z - v_g t$, $t = \tau$ are defined, where v_g is the group velocity which is assumed to be approximately equal to the phase velocity of the excited plasma wave, v_p. The wakefield components can be found from Maxwell's equations.

$$\begin{aligned} \vec{\nabla} \times \vec{E} &= \frac{1}{c}\frac{\partial \vec{B}}{\partial t} \\ \vec{\nabla} \times \vec{B} &= \frac{4\pi}{c}\vec{J} + \frac{1}{c}\frac{\partial \vec{E}}{\partial t}. \end{aligned} \tag{3}$$

Axisymmetric wakefield components can be written as,

$$\frac{\delta E_{wr}}{\delta \xi} - \frac{\delta E_{wz}}{\delta \xi} = \frac{\delta B_{w\theta}}{\delta \xi}, \tag{4a}$$

$$\frac{\delta E_{wr}}{\delta \xi} - \frac{\delta B_{w\theta}}{\delta \xi} = \frac{4\pi}{c} J_r, \tag{4b}$$

$$\frac{\delta E_{wz}}{\delta \xi} = \frac{4\pi}{c} J_z - \frac{1}{r}\frac{\delta(rB_w\theta)}{\delta r}, \tag{4c}$$

E_{wz}, E_{wr}, and $B_{w\theta}$ represent the axial, radial electric wakefields and tangential magnetic field, respectively. J_r and J_z are transverse and axial current density, respectively. It should be mentioned that the second term of Eq. (4c) can be ignored in comparison to the first term; this is due to assuming $B_{w\theta}$ to be slow variation in the transverse direction. With first order perturbative expansion of the electromagnetic field in Eq. (2a) and by using Eq. (1), the first order velocity transverse component of the plasma electron, v_x is obtained as following:

$$\frac{\partial v_x}{\partial \xi} = \frac{e}{mc} E_0 \cos k_0 \xi, \tag{5a}$$

$$v_x = ca \sin k_0 \xi. \tag{5b}$$

The normalized electric field amplitude of the laser pulse is represented by $a = e\ E_0/mc\ \omega_0$. The second order slow axial velocity component of plasma electrons, v_z can be obtained by substituting v_x into Eq. (2a),

$$\frac{\partial v_z}{\partial \xi} = \frac{e}{mc} E_{wz} + \frac{\partial}{\partial \xi}\left(\frac{ca^2}{4}\right). \tag{6}$$

By using $J_z = -n_e\ e\ v_z$ in the partial derivative of Eq. (4c) with respect to ζ and considering Eq. (6) one gets,

$$\left(\frac{\delta^2}{\delta \xi^2} + k_p^2\right) E_{wz} = -\frac{mc^2 k_p^2}{4e}\frac{\delta a^2}{\delta \xi}, \tag{7}$$

k_p is propagation constant of wakefield in plasma. Eq. (7) is the general equation of the produced electric wakefields and can be used for different shapes of the laser pulses. This is due to general assumption of the laser pulse shape in the above calculations. In this work, three fundamental pulse shapes namely, sinusoidal pulse (SP), Gaussian pulse (GP) and rectangular-triangular pulse (RTP) are considered.

Parameter a^2 related to the SP profile is represented by:

$$a^2 = \alpha^2 \sin^2(\pi\xi/L), \quad \alpha = \alpha_0 \exp(-(r/r_0)^2), \tag{8}$$

a^2 is represented for the GP according to,

$$a^2 = a_1^2 \exp\left[-ka_2\left(\xi - \frac{L}{2}\right)^2\right]. \tag{9}$$

https://doi.org/10.1017/S0263034612000195 Published online by Cambridge University Press

The following equation represents parameter a^2 in the RTP.

$$a^2 = \begin{cases} \sqrt{b[1-\cos(2\pi\xi/L)]} & 0 \le \xi \le L/4 \\ \sqrt{b}\left[H\left(\xi-\frac{1}{4}\right)-H\left(\xi-\frac{2L}{3}\right)\right]=\sqrt{b} & L/4 \le \xi \le 2L/3 \\ \sqrt{b\left[\frac{1}{2}+\frac{1}{2}\cos(3\pi\xi/L)\right]} & 2L/3 \le \xi \le L \end{cases} . \quad (10)$$

Where H is the Heaviside unit step function. In Eqs. (8) to (10), α_0, a_1, a_2, and b are constant parameters that calculated to equalize the energy flow of the mentioned three different pulses.

In this work the intensity, angular frequency, and wavelength of laser beam are $I_0 = 1.4\times10^{17}$ Wcm^{-2}, $\omega_0 = 1.88\times10^{15}$ s^{-1}, $\lambda_0 = 1.0$ μm. The density and the wavelength of produced plasma are taken as, $n_0 = 5.32\times10^{18}$ cm^{-3}, $\lambda_p = 15.0$ μm. In order to have same energy flow for the defined three pulses in Eqs. (8) to (10), we have assumed $r = 25$ μm, $r_0 = 4$ μm, $\alpha_0^2 = 0.1$, $a_1^2 = 0.62$, $a_2 = 0.1$, $b = 0.070$.

Eq. (7) is solved using the fourth order Runge-Kutta method by considering the boundary conditions as $E_w(\xi{=}L) = \partial E_w/\partial\xi\ (\xi = L) = 0$ for the mentioned pulses in the region $\zeta \le 0$. The generated wakefield amplitudes behind the pulse shapes are plotted up to the distance $\zeta = 3L$ in Figure 1. Therefore, wakefield amplitudes are 1.27×10^{10}, 0.799×10^{10}, $0.292\times10^{10}(V/m)$ for the RTP, SP, and GP, respectively. The RTP is the most favorable to produce higher amplitude wakefield and larger energy gain of electrons. This is in agreement with the earlier work reported for three pulse shapes, the GP, RGP, and also RTP shapes in a rectangular waveguide (Malik *et al.*, 2007, 2008; Aria *et al.*, 2009).

Considering a second laser pulse copropagating at a distance Δz behind the first pulse. In the beginning of the analytical calculations, the work is treated without any knowledge about the amount of the distance between two pulses. The aim of this study is to generate the optimum wakefield that depends on the optimum distance between two laser pulses inside of plasma, which is achieved as a result of these calculations.

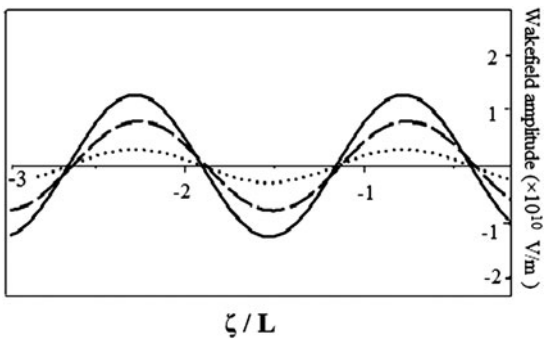

Fig. 1. Wakefield amplitude is generated by the RTP (Solid), SP (Dash), and GP (Dot) shapes in the region $\zeta \le 0$. The maximum wakefield amplitude is related to the RTP.

The electric field vector of the second pulse is given by

$$\vec{E}_s = \hat{x}E_s\cos\{k_0(z-\Delta z)-\omega_0 t\} = \hat{x}E_s\cos\left(k_0\xi'\right), \quad (11)$$

$\xi' = \xi - \Delta z$, and subscript "s" denotes the second pulse. It should be realized that the second pulse has the same intensity, polarization, frequency, length, and flow energy as the first pulse. By using the similar method to the one used for the first pulse (Gaurav *et al.*, 2008) as,

$$\frac{\partial v_{sx}}{\partial\xi} = \frac{e}{mc}E_s,\ \cos k_0\xi', \quad (12a)$$

$$\frac{\partial v_{sx}}{\partial\xi'} = \frac{e}{mc}\left(E_{wz}+E_{swz}\right)+\frac{\partial}{\partial\xi'}\left(\frac{ca_s^2}{4}\right). \quad (12b)$$

In Eq. (12b), a_s is the normalized electric field amplitude of the second pulse and it is $a_s = eE_s/mc\omega_0$.

The axial component of electric wakefield due to the second pulse is given by:

$$\left(\frac{\partial^2}{\partial\xi'^2}+k_p^2\right)E_{swz} = k_p^2E_{wz}-\frac{mc^2k_p^2}{4e}\frac{\partial a_s^2}{\partial\xi'}. \quad (13)$$

The effect of the wakefield generated by the first laser pulse on the wakefield generated by the second laser pulse is considered and the superposition of wakefields of two laser pulses inside of plasma is also calculated according to Eq. (12b). It should be realized that before entering the laser pulse into plasma the superposition can be ignored (Gaurav *et al.*, 2008).

Wakefield amplitude generated behind the second pulse depends on the interpulse separation Δz. By using the mentioned parameters for the laser and plasma and solving Eq. (13) for the SP-SP as a function of Δz, it is found that wakefield amplitude in the region $\xi' \le 0$ changes periodically and one can notice two peaks in Figure 2. In this approach, the same procedure of Eq. (7) is used and the boundary conditions are $E_{sw}(\xi'{=}L) = (\partial E_{sw}/\partial\xi')\ (\xi' = L) = 0$. This figure also indicates a maximum peak at $\Delta z = 0.85\lambda_p$ and this amount is used in plotting of the curves in Figures 3 and 4.

By solving Eq. (13) for the SP-SP, the electric field amplitude of wakefield is plotted up to the distance $\xi'/3L$. It is noticed that if the SP-SP are interred in plasma, the produced wakefield amplitude in first peak is approximately five times greater than the one related to the single SP. Furthermore, in contradict to the single pulse the amplitude of the wakefield produced by two pulses is not constant and it is periodically increasing (see Fig. 3).

One can consider the other arrangements by above mentioned fundamental pulses where, by plotting electric amplitude of wakefield for other dual input pulses, the optimum combination of the laser pulses could be investigated. In Figure 4a, two following combination of pulses are

https://doi.org/10.1017/S0263034612000195 Published online by Cambridge University Press

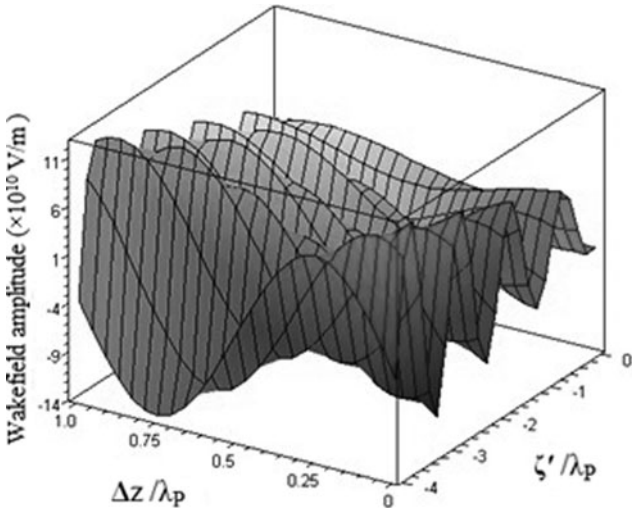

Fig. 2. variation of the wakefield amplitude versus the normalized distance ξ'/λ_p and interpulse separation $\Delta z/\lambda_p$. Generated wakefield amplitude behind the SP-SP which depends on the interpulse separation Δz. Two peaks are observed in its periodical oscillation.

investigated, (1) the RTP-RTP (Dash-Dot), (2) RTP-SP (Dash), and (3) SP-SP (solid). Furthermore, Figure 4b shows two other arrangements of pulses namely, the SP-GP (solid) and SP-RTP (Dash). These Figures show when the first and second pulses were the RTP and SP

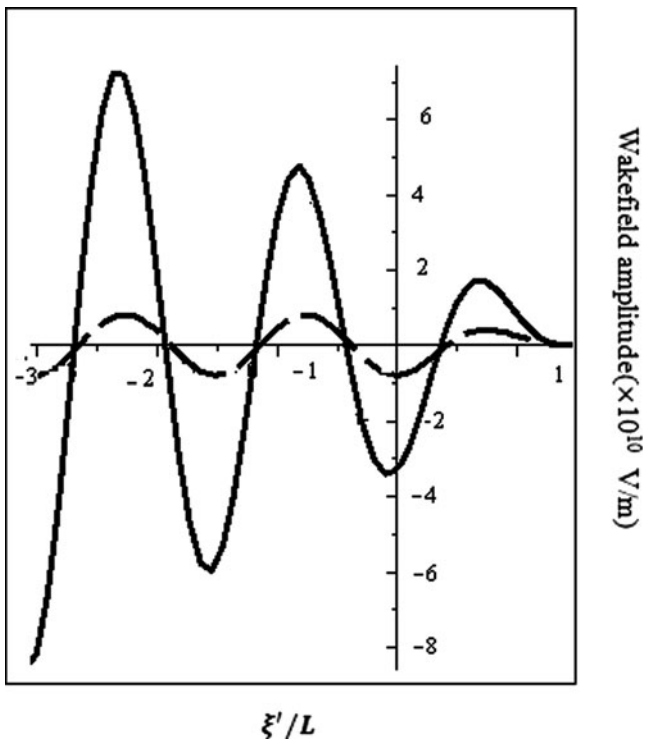

Fig. 3. Wakefield amplitude produced by the SP-SP with interpulse separation $\Delta z = 0.85\lambda_p$ and it is compared with single SP. The amplitude of the SP-SP in the first peak is approximately five times greater than the one generated by the single SP.

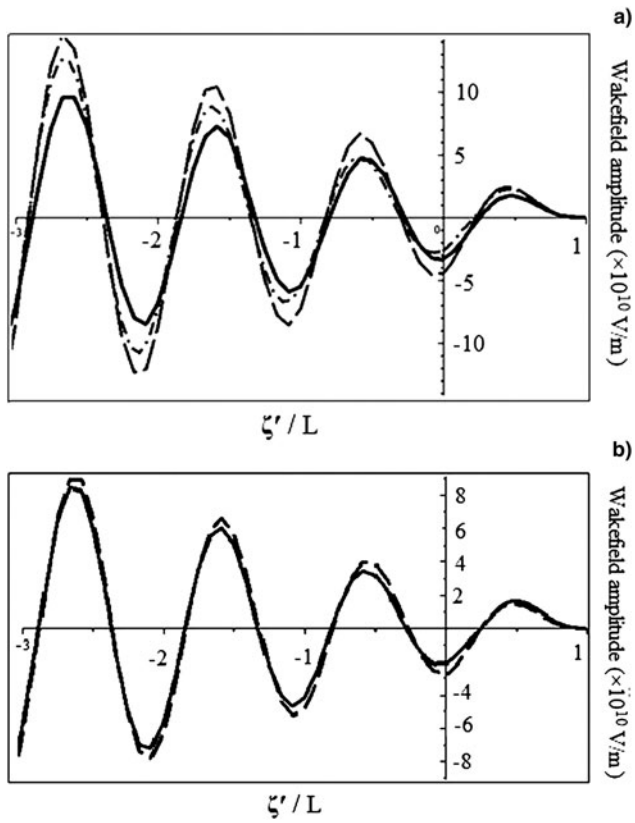

Fig. 4. (**a**) Comparing wakefield amplitude generated by the RTP-RTP (Dash-Dot), RTP-SP (Dash), and SP-SP (solid). It is clear that the RTP-SP has the highest amplitude. (**b**) Comparing wakefield amplitude generated by the SP- RTP (Dash), SP-GP (solid) at the second. It is clear that the SP-RTP has higher amplitude than the SP-GP.

shapes, respectively, wakefield amplitude is peaked and if two pulses are the RTP, the resultant amplitude is greater than the one due the SP-SP. One can notice that the wakefield amplitude depends on both the arrangements and the shape of pulses. In the following, the effect of laser shape pulse on the dissociation of methane is investigated.

THE METHANE

Methane, a symmetrical molecule, constitutes 70% to 95% of natural gas and it is the most stable hydrocarbon at room temperature, which is almost unique on the earth. Methane is recognized as one of the major greenhouse gases with very high global warning potential and it has the highest H/C ratio among hydrocarbons. Methane warms the earth 25 times as much as the same mass of CO_2 (Qin *et al.*, 2007). Each molecule of methane can be directly burned at room temperature by two molecules of oxygen and produce two molecules of water and one molecule of CO_2 with 802 kJ mol^{-1} of heat energy. Although, methane is a clean fuel among other conventional fuels, it has become chemically more valuable when it is converted to the heavier hydrocarbons. The C-H bond of methane needs more energy than

https://doi.org/10.1017/S0263034612000195 Published online by Cambridge University Press

the C-H bond in higher hydrocarbons. This is 12.6 eV, which corresponds to 983 Angstrom and belongs to the vacuum ultraviolet region. The various methane conversion employed techniques include: non-oxidative coupling of methane or aromatization, partial oxidation of methane, reforming by using oxidants milder than oxygen or steam reforming of methane by reacting methane with water molecules, and finally many different catalysts including photocatalysts. For more detail refer to recently presented compressive review in photocatalyst conversion of methane (Cook *et al.*, 2001).

For molecules, some major nonlinear phenomena such as above threshold ionization, field ionization, field assisted dissociation (FAD), coulomb explosion, and explosive photodissociation are reported. Coulomb explosion theory is a widely accepted theory for dissociation dynamics of molecular bonds. In this model, it is very difficult to explain the fragmentation of complex polyatomic molecules due to weaker intermolecular coulomb repulsive force in larger molecules (Cornaggio *et al.*, 1994; Ledingham *et al.*, 1998; Vicente *et al.*, 2000). The highly accepted model is the FAD model introduced by the Wang *et al.* (2003). In the present work, the FAD model is used for calculation of the optimum dissociation probability for the methane ion. The dressed potential energy surfaces of the ground state of the molecular ion and time changes of bond length are calculated by using a Gaussian code at the level of UQCISD/6-31G (Frisch *et al.*, 2003). In the final step, the evaluation of the dissociation probability for single and dual pulse system is done. The introduced approach is a unique process in optimum shaping of the short pulses needed for the dissociation of the desired polyatomic molecules. The ionization of polyatomic molecules is possible with the intensities of about 10^{13} W/cm^2, therefore in this calculation instead of the neutral methane molecule, molecular ion methane CH_4^+, is considered. In the FAD model, the molecule is assumed to be in its ground state and one of its molecular bonding lines is in the direction of the laser pulse. When the molecule is exposed to the laser pulse, only the length of the bond along the laser pulse is changed and other geometry of the molecule is assumed to remain fixed. According to the FAD model polyatomic molecules dissociate spontaneously due to the stretching of their chemical bonds, which is confirmed by the earlier experiments. In the following, the C-H bonding lines of atoms are exposed to the laser pulses as a dual system. The center of mass in CH_4^+ molecule is assumed to be in the central C atom by a good approximation and the distance of H from the center of mass C is noted by q. Time evolution of some parameters such as position, momentum, and width of the Gaussian package is considered by Hamiltonian classical equations. In calculation of the potential energy surfaces with the optional field of the Gaussian package, the phase variation is considered. From Figure 5 one can find that if the C-H bond length q becomes more than 6 Angstrom during the laser exposed time, methane molecule will be dissociated then it can be simulated by gradient

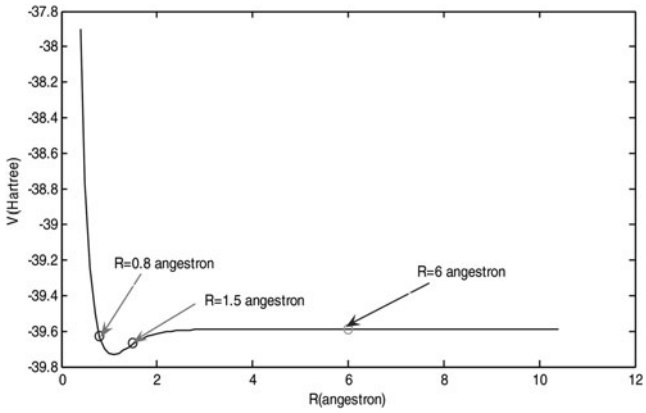

Fig. 5. The potential energy level of the C-H bond of the parent ion CH_4^+. The dissociation distance of C-H bond is also shown.

optimization model and is compared by the variation method (Sundermann *et al.*, 2000).

In this work, by considering the key feature of methane, a new and unique model is presented for optimization of two tailored rectangular femtosecond laser pulses in dissociation of the molecule with maximum probability of one. The main feature of this work is to study the sensitivity of the dissociation probability to the initial bond length q and to control the desired product channel by variation of intensity and time evolution of the laser field via introducing the vector space (I_1, I_2, t_1, t_2, and t_3) with a cost gradient optimization method. In this simple and low cost model, the structural complicacy of solving the related time dependant Schrodinger equation is not needed.

Time evolution of the electric field is given by

$$f(t) = E_0 \sin(\omega t). \tag{14}$$

Where E_0 is amplitude of the electric field and ω is the pulse frequency.

The variation of q and p of a Hamiltonian system with N degrees of freedom are defined by semiclassical initial value representation.

$$\dot{q}_n = \frac{\partial H(p_n, q_n, t)}{\partial p_n}, \dot{p}_n = \frac{-\partial H(p_n, q_n, t)}{\partial q_n}. \tag{15}$$

The Hamiltonian is the sum of kinetic and potential energies. Formally, Using the Poisson bracket, the above equations can be set in to an equation for the phase space vector $\Gamma = (q,p)$

$$\eta^{\bullet} = -\{H, \eta\} = \hat{H}\eta. \tag{16}$$

The equation above is integrated over a small time step, yielding

$$\eta(t + \Delta t) = \exp\{-\Delta t \hat{H}\}\eta(t). \tag{17}$$

By using the high order split-operator procedure in the

https://doi.org/10.1017/S0263034612000195 Published online by Cambridge University Press

semi-classical approach, the effective Hamiltonian is introduced

$$\exp\{-\Delta t\hat{H}_{eff}\} = \exp\left\{\frac{-\Delta t\hat{V}}{2}\right\}\exp\{-\Delta t\hat{T}_k\} \times \exp\left\{\frac{-\Delta T\hat{V}}{2}\right\}. \quad (18)$$

In this numerical calculation, the Hamiltonian splits into the parts representing the kinetic energy and potential energy, where at the first step only the potential part operates, which results in the change of momentum, so called kick step. By considering the new momentum, the position is changed as a drift step. These variations are introduced according to $G = \partial T_k/\partial p$, $F = -\partial V/\partial q$. This procedure is called the variant of the symplectic Euler method. For very short times, this procedure yields

$$q^1 = q^0 + \frac{\Delta tG(p = p^0)}{2}, p^2 = p^0 + \Delta tF(q = q^1), \quad q^2 = q^1 + \frac{\Delta tG(p = p^2)}{2}. \quad (19)$$

In general, any integration model can be expanded to $k = 1,\ldots, n$ in the form of

$$p^k = p^{k-1} + b_k\Delta tF(q^{k-1}), q^k = q^{k-1} + a_k\Delta tG(p^k). \quad (20)$$

Therefore, Δt should be chosen in a way that monitoring the internal movement of the desired molecule is possible. For symmetric molecule of methane, the time duration is suggested to be $\Delta t = 33.75$ (Wang *et al.*, 2003). Therefore, for 2.7 fs laser pulse $T/\Delta T = 2.7\,\text{fs}/33.75 = 80$ and in a sinusoidal field only $80/4 = 20$ first parts of potential is needed. This is because the molecule experiences the same potentials in the last three-quarter of cycles. By manipulation of laser intensity, it is possible to calculate potential by Gaussian 3 code.

In this work, for calculating the dissociation energy of C-H bond of methane 10000 paths are selected by various initial condition. It is supposed that the molecular bond C-H is exposed to a double rectangular laser pulse, which is divided into sinusoidal optical cycles with a period of $T = 2.7$ fs. The initial value of q is selected between 0.8 Angstrom and 1.5 Angstrom and the final value of q is 6 Angstrom, which are reasonable numbers according to Figure 5. In numerical calculations, the time step should be as the same order with as intermolecular vibrational period and one optical cycle is divided by considering the related dressed potential energy surfaces of the bond ground state of the molecular ion. This C-H bond is in the direction of laser field and different laser intensities in each time step is considered by using "field" option in the Gaussian package.

For finding the dissociation probability, time variation of q is calculated for 10000 different trajectories. The difference between the trajectories is because of the selected initial condition in solving the Hamilton equation.

RESULT AND DISCUSSION

As denoted in Figure 5, the first initial condition is that the molecule is in its ground state without feeling any field and q is chosen randomly from the ground state potential well of the molecule. The second initial condition is the velocity of the H atom that is assumed to be zero in a good approximation. The dissociation probability is related to the number of the trajectories ended with a q parameter more than 6 Angstrom for the total number of trajectories. Figures 6 to 9 show the time variation of q and velocity for the mentioned two rectangular laser pulses. From these Figures the importance of the defined initial conditions in obtaining the final magnitude of q can be deduced. In all of these Figures, $I_1 < I_2$ and $t_1 < t_3$, but in Figures 6 and 7 the dissociation of molecule can be seen, while in Figures 8 and 9 the polyatomic molecule is remained in the bond level, because of different initial conditions. In Figure 6, the average bond length is longer than 6 Angstrom, indicating that the molecule has dissociated and optimized dissociation probability is calculated. As a result with characteristic vector $S = (3\times10^{13}\,\text{W/cm}^2,\ 13\times10^{13}\,\text{W/cm}^2,\ 5$ fs, 30 fs, 60 fs) and initial condition $q_0 = 0.72$ Angstrom the maximum probability of 1 is obtained. In Figure 7, showing the time interval of 5 to 35 fs, q is changed by a constant velocity and the applied field is vanished. Therefore, before the termination of laser pulse, the methane ion is dissociated. Continuous enhancement in the momentum is achieved due to the effect of the second pulse after 30 fs delay time. With the new momentum, the bond length is stretched and dissociated. In Figure 8, with the initial condition $q_0 = 0.79$ Angstrom, the average bond length oscillates with time, however, the molecule is remained in the bond level and it cannot be dissociated. In Figure 9, continuous enhancement of the momentum is not observed and the molecule does not have enough energy to dissociate into the products.

For finding the tailored two rectangular laser pulses, we introduced the laser pulse with a characteristic vector S as

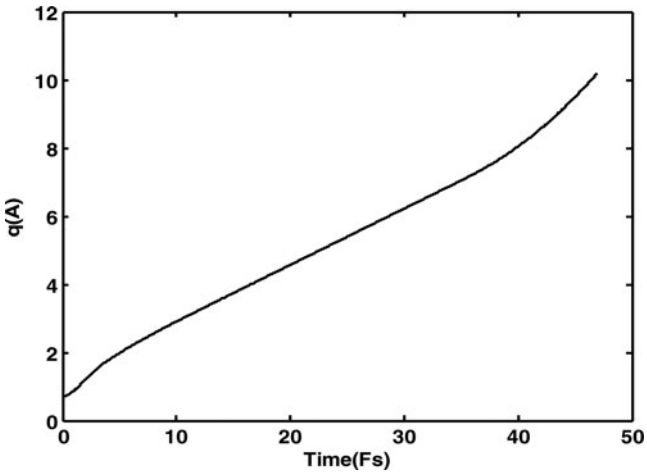

Fig. 6. q versus time for two rectangular laser pulses with characteristic vector $S = (3\times10^{13}\,\text{W/cm}^2,\ 13\times10^{13}\,\text{W/cm}^2,\ 5$ fs, 30 fs, 60 fs) for initial condition $q_0 = 0.72$ Angstrom.

https://doi.org/10.1017/S0263034612000195 Published online by Cambridge University Press

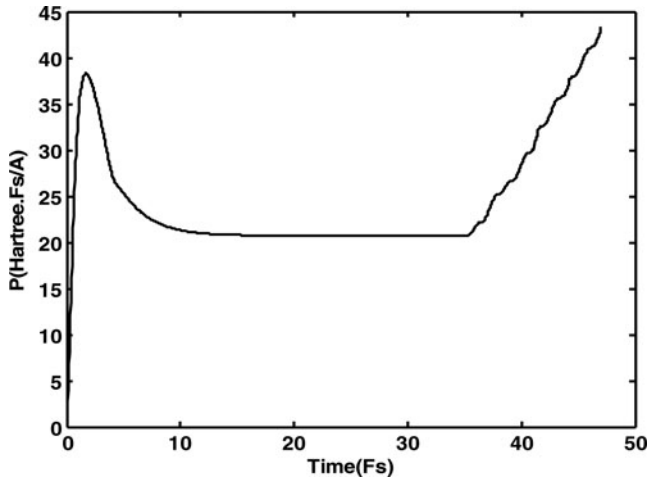

Fig. 7. Velocity versus time for two rectangular laser pulses with characteristic vector $S = (3 \times 10^{13}\ \mathrm{W/cm^2}, 13 \times 10^{13}\ \mathrm{W/cm^2}, 5\ \mathrm{fs}, 30\ \mathrm{fs}, 60\ \mathrm{fs})$ for initial condition $q_0 = 0.72$ Angstrom.

indicated in Figure 10. If the dissociation probability is denoted by p_{diss}, which is assumed to be a function of S then, we try to find the maximum p_{diss} according to the tailored two rectangular laser pulses. The gradient of the S function is in the direction of the local extremes. The goal is to find the two tailored pulse based on the concept of the gradient, of p_{diss}, which can be found by the following equation.

$$\Delta p_{diss} = \begin{bmatrix} \Delta p_{dissI_1} \\ \Delta p_{dissI_2} \\ \Delta p_{disst_1} \\ \Delta p_{disst_2} \\ \Delta p_{disst_3} \end{bmatrix} = \begin{bmatrix} \dfrac{p_{diss}(I_1 \pm dI_1) - p_{diss}(I_1)}{dI_1} \\ \dfrac{p_{diss}(I_2 \pm dI_2) - p_{diss}(I_2)}{dI_2} \\ \dfrac{p_{diss}(t_1 \pm dI_1) - p_{diss}(t_1)}{dI_1} \\ \dfrac{p_{diss}(t_2 \pm dI_2) - p_{diss}(t_2)}{dI_2} \\ \dfrac{p_{diss}(t_3 \pm dI_3) - p_{diss}(t_3)}{dI_3} \end{bmatrix}. \quad (21)$$

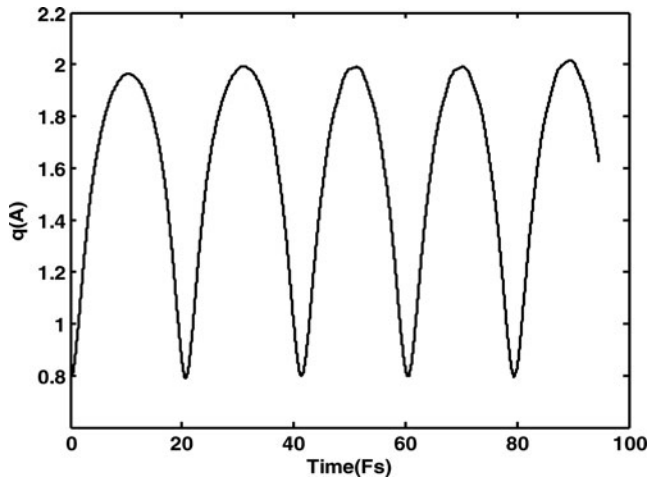

Fig. 8. q versus time for two rectangular laser pulses with characteristic vector $S = (3 \times 10^{13}\ \mathrm{W/cm^2}, 13 \times 10^{13}\ \mathrm{W/cm^2}, 5\ \mathrm{fs}, 30\ \mathrm{fs}, 60\ \mathrm{fs})$ for initial condition $q_0 = 0.79$ Angstrom.

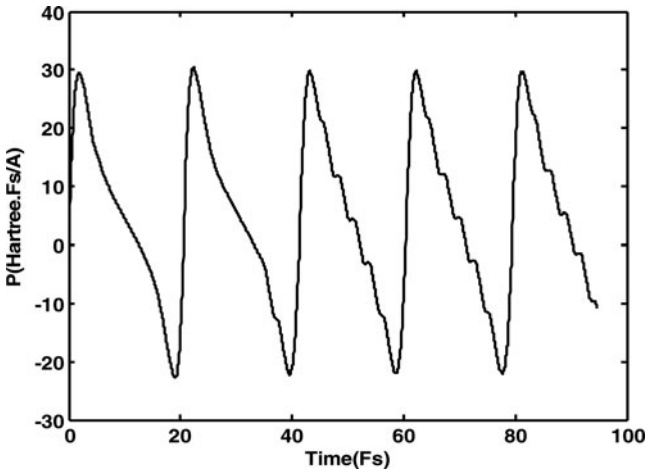

Fig. 9. Velocity versus time for two rectangular laser pulses with characteristic vector $S = (3 \times 10^{13}\ \mathrm{W/cm^2}, 13 \times 10^{13}\ \mathrm{W/cm^2}, 5\ \mathrm{fs}, 30\ \mathrm{fs}, 60\ \mathrm{fs})$ for initial condition $q_0 = 0.79$ Angstrom.

Following ∇p_{diss} calculation, the next step is moving toward its direction determination in the produced space by the parameters of the characteristic vector S. This step is shown by the following equation:

$$\begin{bmatrix} I_1 \\ I_2 \\ t_1 \\ t_2 \\ t_3 \end{bmatrix}_{Next} = k\Delta p_{diss} + \begin{bmatrix} I_1 \\ I_2 \\ t_1 \\ t_2 \\ t_3 \end{bmatrix}_{Initial}. \quad (22)$$

We choose k as a random integer less than 10 in each optimization step. The energy of the laser pulse or area under the intensity-time curve should be fixed. For more simplification, we suppose that t_2 and the total energy of the two rectangular pulses i.e., $E = I_1 t_1 + I_2 t_3$ are assumed to be fixed. Then, the degree of freedom will be reduced to three and it will make the calculations less complicated. Our space optimization shown in Figure 11 is built by considering the constraint and choosing proper boundaries for the variables.

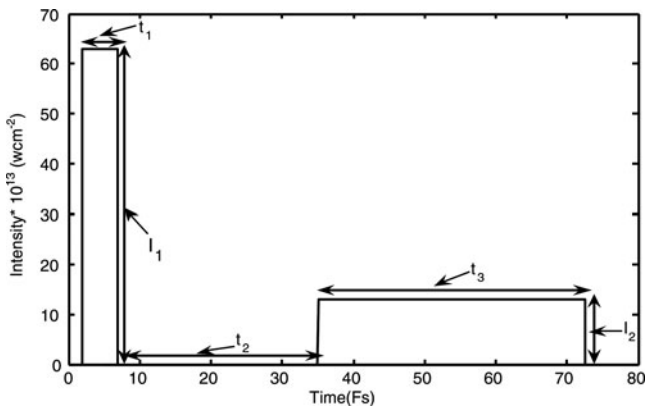

Fig. 10. Two rectangular laser pulses is introduced by a characteristic vector space S = (I_1, I_2, t_1, t_2, t_3).

https://doi.org/10.1017/S0263034612000195 Published online by Cambridge University Press

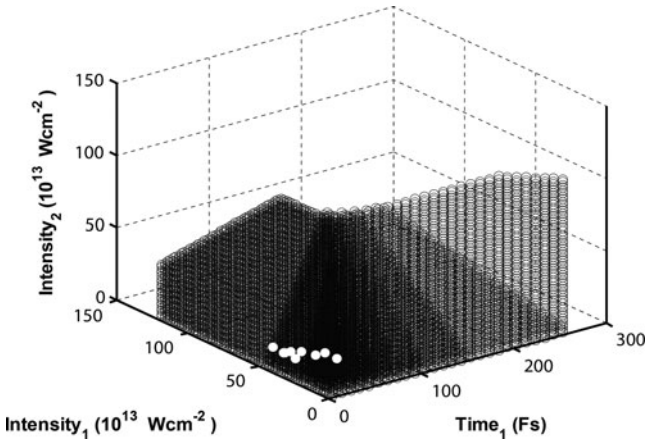

Fig. 11. The optimization space is shown. The white circles show the some of the optimized points and the optimization trajectory.

Based on the mentioned constraints it is found that the laser pulse intensities are in the range of I_1, $I_2 \in [1, 121] \times 10^{13}$ W/cm^2 and t_1, $t_3 \in [5, 255]$ fs.

The Table 1 shows the resulting pulses for providing the dissociation probability of one. Calculations performed for one rectangular pulse by FAD models show that the dissociation will saturate at a certain pulse width.

In this calculation, several S vectors are found and saturation in dissociation can be shown when a molecule is exposed by two rectangular laser pulses. For all proper tailored pulses, it is found that $I_1 > I_2$. Classically, it is because the initial acceleration of H atom is high and it is caused that q to reach to the length of 6 Angstrom immediately. When the molecule is exposed to the second part of the laser pulse, it is not in the potential well of the molecular bond. Therefore, the intensity effect of the second part of the laser pulse seems to be less important than the first part. The molecule may be exposed to a laser pulse, which its first part of it has less intensity and the second part generates a high acceleration in the H atom. In this case, in spite of the high acceleration of H atom, the laser energy constrain does not have enough time to reach to a required bond length. This is in agreement with the earlier result reported by Wang *et al.* (2006) that is pertinent to the rectangular pulse. They found experimentally that below a certain laser pulse, the bond width in spite of the high intensity of the laser pulse, the dissociation of molecular ion was not observed.

Table 1. *The obtained results shown in the table indicate that the first pulse is more intensive than the second pulse.*

$I_1(10^{13}$ Wcm$^{-2})$	$I_2(10^{13}$ Wcm$^{-2})$	t_1 (fs)	t_3 (fs)
55	19	5	27.6
63	13	5	37.3
49	11	15	5.9
49	13	15	5

CONCLUSION

In the present work, three fundamental profiles of pulses are used to find the maximum generated wakefield amplitude. It is found that wakefield amplitude induced by RTP is greater than the wakefield of others combinations. Moreover, to find the optimum wakefield amplitude produced by dual trailing laser pulses four different arrangements are considered in plasma. It is noticed that when the first and second pulses were the RTP and SP shapes respectively, the resultant wakefield amplitude is maximum. This achievement can have good impact in controlling of chemical reactions in the desired channels by short pulse intense lasers for reducing the computation time of genetic algorithm model. In addition, a simple and very useful method is introduced for the first time to produce optimized two tailored rectangular laser pulses which dissociates the molecular ion CH_4^+ with the maximum probability of one. This optimization analyzes some information about the molecular dynamics which should describe the control of a bulk sample of molecules at different positions. Furthermore in this model we achieve the best initial q with the maximum dissociation probability and possibility of the laser wavelength tuning to match the vibrational frequencies of the different pathways. In these calculations, the advanced FAD model by using a semiclassical view and the gradient optimization method is used. The molecular bond is assumed to be in the same direction of the laser electric field. These calculations can be improved by assuming that there are molecular bonds not in the same direction as the electric field, which feel the laser effect (Wang *et al.*, 2006). Saturation for dissociation of the mentioned molecular bond is found, where the first rectangular pulse should have higher intensity than the second one. Analysis of the pulses resulting in selective control is with the maximum product yield and less complexity. Also these results can reduce the costs of obtaining an optimized pulse shape needed for controlling the chemical reactions.

ACKNOWLEDGMENTS

The authors want to thank Pars oil and gas company of ministry of oil for their support of this project through contract number PT131. We also acknowledge the research deputy of Sharif University of Technology.

REFERENCES

Aria, A.K., Malik, H.K. & Singh, K.P. (2009). Excitation of wakefield in a rectangular waveguide: Comparative study with different microwave pulses. *Laser Part. Beams* **27**, 41–47.

Assion, A., Baumert, T., Bergt, M., Brixner, T., Kiefer, B., Seyfried, F., Strehle, M. & Gerber, G. (1998*a*). Evolutionary algorithms and their application to optimal control studies. *Sci.* **282**, 91.

Assion, A., Baumert, T., Bergt, M., Brixner, T., Kiefer, B., Seyfried, V., Strehle, M., Gerber, G. (1998*b*). Control of

https://doi.org/10.1017/S0263034612000195 Published online by Cambridge University Press

chemical reactions by feedback-optimized phase-shaped femtosecond laser pulses. *Sci*. **282**, 919.

Balakirev, V.A., Karas, V.I., Karas, I.V. & Levchenko, V.D. (2001). Plasma wakefield excitation by relativistic electron bunches and charged particle acceleration in the presence of external magnetic field. *Laser Part. Beams* **19**, 597–604.

Bauer, D. (2002). Molecules and clusters in intense laser field. *Laser Part. Beams* **20**, 541–542.

Bauer, D. (2003). Plasma formation through field ionization in intense laser–matter interaction. *Laser Part. Beams* **21**, 489–495.

Bauer, D. & Ceccherini, F. (2001). A numerial ab initio study of harmonic generation from a ring shaped model molecule in laser fields. *Laser Part. Beams* **19**, 85–90.

Bessonov, E.G., Gorbunkov, M.V., Ishkhanov, B.S., Kostryukov, P.V., Maslova, Yu.Ya., Shvedunov, V.I., Tunkin, V.G. & Vinogradov, A.V. (2008). Laser-electron generator for X-ray applications in science and technology. *Laser Part. Beams* **26**, 489–495.

Bostandoust Nik, E. & Sadighi-Bonabi, R. (2010). Theoretical study of CO adsorption on the illumnated TiO_2(001) surface. *Appl. Surf. Sic*. **256**, 3795–3798.

Brumer, P. & Shapiro, M. (2009). Quantum coherance in the control of molecular processes. *Laser Part. Beams* **16**, 599–603.

Castro, A. & Gross, E.K.U. (2009). Acceleration of quantum optimal control theory algorithms with mixing strategies. *Phys. Rev. E* **79**, 056704.

Chyla, W.T. (2006). On generation of collimated highpower gamma beams. *Laser Part. Beams* **24**, 143–156.

Cook, P.A., Ashfold, M.N.R., Jee, Y.J., Jung, K.H., Harich, S. & Yang, X. (2001). Vaccum ultra-violet photochemistry of methane. Silane and germane. *Phys. Chem. Chem. Phys*. **3**, 1848–1860.

Cornaggio, C., Schmidt, M. & Normand, D. (1994). Coulomb explosion of CO_2 in an intense femto-second laser field. *J. Phys. B* **27**, 123.

Cowan, T.E., Perry, M.D., Key, M.H., Ditmire, T.R., Hatchett, S.P., Henry, E.A., Moody, J.D., Moran, M.J., Pennington, D.M., Phillips, T.W., Sangster, T.C., Sefcik, J.A., Singh, M.S., Snavely, R.A., Stoyer, M. A., Wilks, S.C., Young, P.E., Takahashi, Y., Dong, B., Fountain, W., Parnell, T., Johnson, J., Hunt, A.W. & Kühl, T. (1999). High energy electrons, nuclear phenomena and heating in petawatt laser-solid experiments. *Laser Part. Beams* **17**, 773–783.

Dyson, A. & Dangor, A.E. (1991). Laser beat wave acceleration of particles. *Laser Part. Beams* **9**, 619–631.

Frisch, M.J., Trucks, G.W., et al. (2003). Gaussian03, Revisiona.1, Gaussian, Pittsburgh, Pa. Goswami, D. *Phys. Rep*. 374–385.

Gaurav, R., Ajay, K.U., Rohit, K.M. & Pallavi, J. (2008). Electron acceleration by two copropagating laser pulses in plasma. *Phys. Rev. Accel. Beams* **11**, 071301.

Giulietti, D., Galimberti, M., Giulietti, A., Gizzi, L.A., Labate, L. & Tomassini, P. (2005). The laser-matter interaction meets the high energy physics Laser-plasma accelerators and bright X/γ-ray sources. *Laser Part. Beams* **23**, 309–314.

Glinec, Y., Faure, J., Pukhov, A., Kiselev, S., Gordienko, S., Mercier, B. & Malka, V. (2005). Generation of quasi-monoenergetic electron beams using ultrashort and ultraintense laser pulses. *Laser Part. Beams* **23**, 161–166.

Glowacz, S., Hora, H., Badziak, J., Jablonski, S., Cang, Yu. & Osman, F. (2006). Analytical description of rippling effect and ion acceleration in plasma produced by a short laser pulse. *Laser Part. Beams* **24**, 15–25.

Graham, P., Fang, X., Ledingham, K.W.D., Sinohal, R.P., Mccanny, T., Smith, D.J., Kosmidis, C., Tzallas, P. & Langeley, A.J. (2000). Unusual fragmentation pattern from the dissociation of small molecule. *Laser Part. Beams* **18**, 417–432.

Graham, P., Menkir, G. & Levis, R.J. (2003). An investigation of the effects of experimental paremeters on the closed loop control of photoionization, dissociation processes in acetophenone. *Spec. Chim. Acta B* **58**, 1097.

Hoffmann, D.H.H., Blasevic, A., Rosmej, P.N.I., Roth, M., Tahir, N.A., Tauschwitz, A., Udera, S., Vanentsov, D., Weyrich, K. & Maron, Y. (2005). Present and future perspectives for high energy density physics with intensive heavy ion and laser beams. *Laser Part. Beams* **23**, 47–53.

Hora, H. (2004). Developments in inertial fusion energy and beam fusion at magnetic confinement. *Laser Part. Beams* **22**, 439–449.

Hora, H. (2007). New aspects for fusion energy using inertial confinement. *Laser Part. Beams* **25**, 37–46.

Hora, H. (2009). Laser fusion with nonlinear force driven plasma blocks: Thresholds and dielectric effects. *Laser Part. Beams* **27**, 207–222.

Hornung, T., Meier, R., Zeidler, D., Kompa, K.L., Proch, D. & Motzkus, M. (2000). Optimal control of one-and two photon transitions with shaped femtosecond pulses and feedback. *Appl. Phys. B* **71**, 277–284.

Jiang, Z., Learird, D.E. & Weiner, A.M. (2005). Line by line pulse shaping control for optical arbitrary waveform generation. *Opt. Exp*. **13**, 25.

Judson, R.S. & Rabitz, H. (1992). Teaching lasers to control molecules. *Phys. Rev. Lett*. **68**, 1500–1503.

Leemans, W.P., Catravas, P., Esarey, E., Geddes, C.G.R., Toth, C., Trines, R., Schroeder, C.B. & Shadwick, B.A. (2002). Electron-yield enhancement in a laser-wakefield accelerator driven by asymmetric laser pulses. *Phys. Rev. Lett*. **89**, 174802.

Lifschitz, A.F., Faure, J., Glinec, Y., Malka, V. & Mora, P. (2006). Proposed scheme for compact GeV laser plasma accelerator. *Laser Part. Beams* **24**, 255–259.

Malik, H.K., Kumar, S. & Singh, K.P. (2008). Electron acceleration in a rectangular waveguide filled with unmagnetized inhomogeneous cold plasma. *Laser Part. Beams* **26**, 197–205.

Malik, H.K., Kumar, S. & Nishida, Y. (2007). Electron acceleration by laser produced wakefield: Pulse shape effect. *Opt. Commun*. **280**, 417–423.

Malka, V. & Fritzler, S. (2004). Electron and proton beams produced by ultra short laser pulses in the relativistic regime. *Laser Part. Beams* **22**, 399–405.

Maslova, Yu.Ya., Shvedunov, V.I., Tunkin, V.G. & Vinogradov, A.V. (2008). Laser-electron generator for X-ray applications in science and technology. *Laser Part. Beams* **26**, 489–495.

Nikzad, L., Sadighi-Bonabi, R., Riazi, Z., Mohammadi, M. & Heydarian, F. (2012). Simulation of enhanced characteristic X-rays from a 40-MeV electron beam laser accelerated in plasma. *Phys. Rev. Accel. Beams* **15**, 021301.

Oron, D., Dudovich, N. & Silberberg, Y. (2003). Femtosecond phase-and-polarization control for background free coherent anti stocks Raman spectroscopy. *Phys. Rev. Lett*. **90**, 21.

Oron, D. & Silberg, Y. (2005). Spatio temporal coherent control using shaped temporally focused pulses. *Opt. Exp*. **13**, 24.

Perlado, J.M., Sanz, J.,Velarde, M., Reyes, S., Caturla, M.J., Arévalo, C., Cabellos, O., Dominguez, E., Marian, J., Martinez, E., Mota, F., Rodriguez, A., Salvador, M. & Velarde, G. (2005). Activation and damage of fusion materials and tritium effects in inertial fusion reactors: Strategy for adequate irradiation. *Laser Part. Beams* **23**, 345–349.

Rabitz et al. (1988). *Phys. Rev. A* **37**, 4950.

Rosenzweig, J.B., Cline, D.B., Cole, B., Figueroa, H., Gai, W., Konecny, R., Norem, J., Schoessow, P. & Simpson, J. (1988). Experimental observation of plasma wakefield acceleration. *Phys. Rev. Lett*. **61**, 98–101.

Roth, M., Brambrink, E., Audebert, B., Blazevic, A., Clarke, R., Cobble, J., Cowan, T.E., Fernandez, J., Fuchs, J., Geissel, M., Habs, D., Hegelich, M., Karsch, S., Ledingham, K., Neely, D., Ruhl, H., Schlegel, T. & Schreiber, J. (2005). Laser accelerated ions and electron transport in ultra-intense laser matter interaction. *Laser Part. Beams* **23**, 95–100.

Sadighi-Bonabi, R. & Etehadi-Abari, M. (2010*d*). The electron density distribution and field profile in underdense magnetized plasma. *Phys. Plasmas* **17**, 032101.

Sadighi-Bonabi, R. & Kokabi, O. (2006). Evaluation of transmutation of ^{137}Cs (γ, n) ^{136}Cs using ultra intense lasers. *Ch. Phys. Lett*. **6**, 1434–1436.

Sadighi-Bonabi, R. & Moshkelgosha, M. (2011). Self-focusing up to the incident laser wavelength by an appropriate density ramp. *Laser Part. Beams* **29**, 453–458.

Sadighi-Bonabi, R. & Rahmatollahpur, Sh. (2010*e*). Potential and energy of the monoenergetic electrons in an alternative ellipsoid bubble model. *Phys. Rev. A* **81**, 023408.

Sadighi-Bonabi, R. & Rahmatollahpur, Sh. (2010*f*). A complete accounting of the monoenergetic electron parameters in an ellipsoidal bubble model. *Phys Plasmas* **17**, 033105.

Sadighi-Bonabi, R., Habibi, M. & Yazdani, E. (2010*h*). Improving the relativistic self-focusing of intense laser beam in plasma using density transition. *Phys. Plasmas* **16**, 083105.

Sadighi-Bonabi, R., Habibi, M. & Yazdani, E. (2009*b*). Improving the relativistic self-focusing of intense laser beam in plasma using density transition. *Phys. Plasmas* **16**, 083105.

Sadighi-Bonabi, R., Hora, H., Riazi, Z., Yazdani, E. & Sadighi, S.K. (2010*a*). Generation of plasma blocks accelerated by nonlinear forces from ultraviolet KrF laser pulses for fast ignition. *Laser and Particle Beams* **28**, 101–107.

Sadighi-Bonabi, R., Irani, E., Safaie, B., Imani, Kh. Silatani, M. & Zare, S. (2010*c*). Possibility of ultra-intense laser transmutation of ^{93}Zr (γ, n) ^{92}Zr a long-lived nuclear waste into a stable isotope. *Energy Conver. Manag*. **51**, 636–639.

Sadighi-Bonabi, R., Navid, H. A. & Zobdeh, P. (2009*a*). Observation of quasi mono-energetic electron bunches in the new ellipsoid cavity model. *Laser Part. Beams* **27**, 223–231.

Sadighi-Bonabi, R., Rahmatallahpor, S., Navid, H.A., Lotfi, E., Zobdeh, P., Reiazi, Z., Nik, M.B. & Mohamadian, M. (2009*c*). Modification of the energy of mono-energetic electron beam by ellipsoid model for the cavity in the bubble regime. *Contrib. Plasma Phys*. **49**, 49–54.

Sadighi-Bonabi, R., Yazdani, E., Cang, Y. & Hora, H. (2010*g*). Dielectric magnifying of plasma blocks by nonlinear force acceleration with delayed electron heating. *Phys. Plasmas* **17**, 113108.

Sadighi-Bonabi, R., Yazdani, E., Cang, Y. & Hora., H. (2010*b*). Dielectric magnifying of plasma blocks by nonlinear force acceleration with delayed electron heating. *Phys. Plasmas* **17**, 113108.

Sadighi-Bonabi, R.,Yazdani, E., Habibi, M. & Lotfi, E. (2009*d*). Comment on "Plasma Density Ramp for Relativistic Self-focusing of an Intense Laser. *J. Opt. Soc. Am. B* **27**, 1731.

Sprangle, P., Esarey, E. & Ting, A. (1990). Nonlinear theory of intense laser-plasma interactions. *Phys. Rev. Lett*. **64**, 2011–2014.

Sprangle, P., Hafizi, B., Peñano, J.R., Hubbard, R.F., Ting, A., Moore, C.I., Gordon, D.F. , Zigler, A., Kaganovich, D., Antonsen Jr., T.M., (2001). Wakefield generation and GeV acceleration in tapered plasma channels. *Phys. Rev. E* **63**, 056405.

Sugimori, K., Ito, T., Takta, Y., Ichitani, K., Nagao, H. & Nishikawa, K. (2007). Theoretical study of above- threshold dissociation on diatomic molecules by using nonresonant intense laser pulses. *J. Phys. Chem. A* **111**, 9417–9423.

Sundermann, K., Rabitz, H. & Vivie-Riedle, R. (2000). Compensating for spatial laser profile effects on the control of quantum systems. *Phys. Rev. A* **62**, 013409.

Vicente, J.J., Ferconiand, A.M. & Pantelipes, S.T. (2000). Interactions of intense radiation with atoms, molecules and solids. *Laser Part. Beams* **18**, 557–562.

Wang, C., Song, D., Liu, Y. & Kong, F. (2006). Pulse width effect on the dissociation probability of CH4+ in the intense femtosecond laser field. *Chinese Science Bulletin* **51**, 10.

Wang, S., Tang, X., Gao, L., Elshakre, M. & Kong, F. (2003). Dissociation of methane in intense laser fields. *J. Phys. Chem. A* **107**, 32.

Yazdani, E., Cang, Y., Sadighi-Bonabi, R., Hora, H. & Osman, F.H. (2009). Layers from initial Rayleigh density profile by directed nonlinear force driven plasma blocks for alternative fast ignition. *Laser Part. Beams* **27**, 149–156.

Zewail, A.H. (1994). *Femto chemistry*. World scientific.

Zobdeh, P., Sadighi-Bonabi, R. & Afarideh, H. (2008). New ellipsoid cavity model for high-intensity laser-plasma interaction. *Plasma Dev. Oper*. **16**, 105–114.

Zobdeh, P., Sadighi-Bonabi, R. & Afarideh, H. (2010). Electron trajectory evaluation in laser-plasma interaction for effective output beam. *Chin. Phys. B* **19**, 064210.